PLASMAS AND GASES

O.M. KORBUT, V.A. KELMAN, YU.V. ZHMENYAK, M.S. KLENIVSKYI

Institute of Electron Physics, Nat. Acad. of Sci. of Ukraine
(21, Universytets'ka Str., Uzhgorod 88017, Ukraine; e-mail: vkel171@gmail.com)

EMISSION PROPERTIES OF AN ATMOSPHERIC PRESSURE ARGON PLASMA JET EXCITED BY BARRIER DISCHARGE

PACS 50.20.Dg

An atmospheric-pressure argon plasma jet is initiated by the barrier discharge in a capillary, through which argon was flown. The spectral composition of radiation emitted by the jet in the atmosphere and its variation in the space are analyzed in detail. The jet radiation spectrum is shown to be predominantly formed by spectral transitions of argon and oxygen atoms, by electron-vibrational transitions of the first positive system of nitrogen molecules N_2 $(C\ ^3\Pi_u \to B\ ^3\Pi_g)$, and by transitions of hydroxyl radical $OH(A\ ^2\Sigma^+ \to X\ ^2\Pi)$.

K e y w o r d s: plasma jet, barrier discharge, radiation spectrum, spatial distribution of radiation.

1. Introduction

A considerable attention of researchers has been attracted recently to low-power atmospheric pressure plasma jets initiated by low-current discharge [1]. Unlike the plasma jets generated by high-current arc discharges, the low-current plasma of atmospheric-pressure gas-discharge jets is strongly nonequilibrium, because the temperature of its electrons exceeds the gas temperature by orders of magnitude. This method of plasma generation practically does not result in the heating of the gas component of a plasma, so that the gas temperature in a plasma remains at a level of room one. While interacting with various materials and objects, the "cold" gas jet does not damage them thermally, which opens wide specific domains of application for such plasma.

The nonequilibrium atmospheric-pressure plasma has a wide spectrum of applications in such intensively developing directions as the treatment and cleaning of material surfaces [2–4], sputtering of coatings [5, 6], etching [7, 8], sterilization [9, 10], biomedicine [11–13], surgery [14], stomatology [15–17] and

others. In particular, the plasma jet is successfully applied in stomatology to treat caries-affected teeth before their filling owing to the strong bactericidal action of a plasma [18, 19]. In addition, this treatment enhances the adhesion of the sealer to the tooth tissue and prolongs the filling durability [20, 21].

The atmospheric-pressure plasma is known to be one of the most effective sterilization sources [22], with helium being the major working gas used at its generation. However, plasma jet sources of this kind consume a considerable amount of helium, which is an expensive inert gas. The temperature of a helium plasma jet at the capillary output reaches 150 °C and can damage the analyzed surface. Therefore, the authors of work [22] proposed to replace helium by argon as a working gas. According to the results in [23, 24], the electron concentration in an argon plasma exceeds that in a helium plasma by a factor of 2–2.5. If oxygen, O_2, is used as the active gas in a jet together with argon, the plasma can produce other particles, such as $O(^3P)$, $O^*(^1D)$, $O_2^*(^1\Delta_g)$, and others. In addition, the argon-based plasma jet deeply penetrates into the atmospheric air, which favors the creation of a path for oxygen radicals that sterilize the examined surface. In work [24], it was shown that a high

efficiency of the surface sterilization from microbes can be attained with the help of a plasma jet on the basis of the argon–oxygen gas mixture. The efficiency depends on the oxygen concentration in the argon plasma. Such plasma can effectively sterilize a surface from microbes at relatively low temperatures, which considerably diminishes the degree of thermally induced damage at rather small amounts of argon [25]. The work of sterilizers on the basis of the barrier discharge in the atmospheric gas with various humidity levels was studied in works [26, 27] in detail. The authors of those works obtained a good agreement between the results of experimental measurements and model calculations of the plasma composition in both the discharge volume and a working chamber for the sterilization of materials.

A wide scope of applications of the atmospheric-pressure gas-plasma jets stimulates the development of new sources with various working gases, as well as comprehensive researches of their work. In particular, the information on the spectral and spatial distributions of radiation emitted by plasma jets and the physics of processes in discharge plasma is of interest.

Some important results concerning the kinetics of processes in the argon–nitrogen plasma of a glow discharge were obtained in works [28, 29], which confirmed the crucial role of atomic nitrogen in the processes of metal surface nitriding. This work is aimed at analyzing the work of a source generating a "cold" atmospheric-pressure argon plasma jet excited by a barrier discharge. The spatial and spectral distributions of its radiation intensity are also studied.

2. Experimental Equipment and Method

For carrying out the researches, a discharge unit containing a quartz capillary 50 mm in length with an internal diameter of 3 mm and an external one of 6 mm had been designed and constructed. The geometry and the positions of electrodes in the discharge unit corresponded to the barrier type of a discharge. Inside the capillary, there was an electrode in the form of a sharpened rod 2.3 mm in diameter and 45 mm in length. The other electrode fabricated in the form of a foil strip 25 mm in width was coiled around the capillary, so that the cylindrical wall of the latter played the role of a dielectric barrier between the electrodes. The gap between the electrodes was equal to 1.85 mm, 1.5 mm of which were occupied by quartz insulator. The distance from the electrodes

to the capillary cut amounted to 7 mm. The inert gas argon was blown through the capillary. The argon consumption was approximately 1.7 l/min, and the flow velocity of inert gas atoms at the capillary output was evaluated to equal 1 m/s.

The choice of a barrier discharge for the gas excitation was associated, in particular, with the fact that the barrier discharge is related to low-power low-current discharges and induces no substantial heating of the gas component in a generated plasma. The presence of a dielectric barrier provided a restriction on the amount of electric energy that was introduced into the discharge during an excitation pulse and was governed by the interelectrode capacitance.

The discharge was excited in the capillary with the help of high-voltage unipolar pulses with a repetition frequency of 2.5 kHz. The pulse voltage source was designed according to the circuit of resonance charging of a 825-pF reservoir capacitor from a high-voltage rectifier followed by its discharge with the help of a thyratron commutator TGI1-2000/35. The experimental voltage at a rectifier was 1.1 kV, and the average discharge current was 0.08 A.

The spectral distribution of the discharge radiation intensity was studied with the help of a diffraction monochromator MS 7504i designed according to the Czerny–Turner horizontal optical scheme. A CCD camera HS 101H with a 2048×122-pixel matrix was used as a photorecording detector. A signal from a CCD camera was supplied to a personal computer for the registration and the further processing. While determining the spatial distribution of the radiation intensity, the space coordinate was scanned by moving the focusing lens along the jet in parallel to the plane of the monochromator input slit.

Besides the spectral characteristics of an argon plasma jet, the time parameters of the pulse radiation emission by plasma components were analyzed with the help of a registration system consisting of a monochromator MDR-6, a photodetector FEU-106, and an oscilloscope S1-99. The general schematic diagram describing the excitation of barrier discharge, the formation of plasma jet, and the experimental setup is depicted in Fig. 1.

3. Results of Researches and Their Discussion

When a pulse-periodic high voltage was applied to the electrodes of the gas-discharge quartz capillary, through which the inert gas argon was blown, a

plasma jet, which looked like a needle-shaped torch with a characteristic lilac tint, started to burn in the air. This tint was associated, as will be shown below, with the domination of the spectral lines of argon, which was mixed up in the capillary with the air components, in the radiation spectrum of the discharge plasma. Beyond the output capillary cut, the plasma jet length was visually evaluated to equal about 10 mm.

In the course of researches, the spectral composition of radiation emitted by the argon plasma jet formed in the atmosphere was studied. The integrated-over-time radiation spectrum of the discharge plasma in the wavelength interval 280–790 nm is exhibited in Fig. 2. Even a quick look is enough to understand that it consists of two emission groups: a short-wave group (300–406 nm), which contains the bands in the ultra-violet and violet spectral ranges, and a long-wave one (696–922 nm), which contains the bands in the red and IR spectral ranges.

A detailed analysis of the discharge radiation spectrum brought us to a conclusion that the main emitting components in a plasma jet, besides the inert gas argon blown through the capillary, are nitrogen, oxygen, and hydroxyl radicals. The presence of the emission lines of nitrogen and oxygen molecules, besides those of the inert gas argon, in the discharge radiation spectrum is caused by the accompanying excitation of atmospheric gases in the air, because the discharge burned in a direct contact with the latter. The radiation emission by excited hydroxyl radicals takes place owing to their formation as a result of the dissociation of water molecules, which are present in air in the form of an atmospheric moisture and as an admixture to argon.

The most intense spectral emissions among the registered ones of the studied argon plasma jet, as well as their identification, are quoted in Table. The atomic spectral lines in the emission spectrum were identified with the help of reference data [30, 31], and the vibrational transitions of molecular components in the discharge plasma were determined on the basis of the results of works [32, 33].

In the long-wave (red) spectral interval of the discharge radiation spectrum (690–922 nm), the lines of spectral transitions $3p^5 4p \rightarrow 3p^5 4s$ and $3p^5 4d \rightarrow 3p^5 4p$ between the excited states of argon atoms were registered, which are mainly responsible for tinting the plasma jet in lilac. The emission of argon spectral
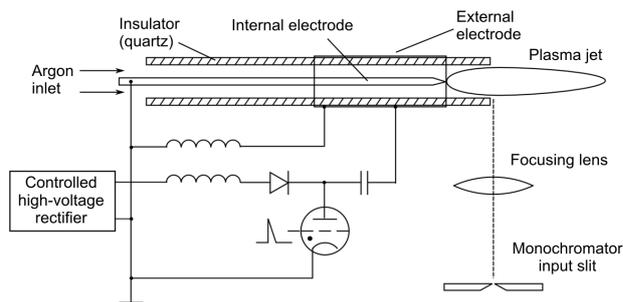

Fig. 1. Schematic diagram of the barrier discharge excitation, plasma jet formation, and experimental equipment
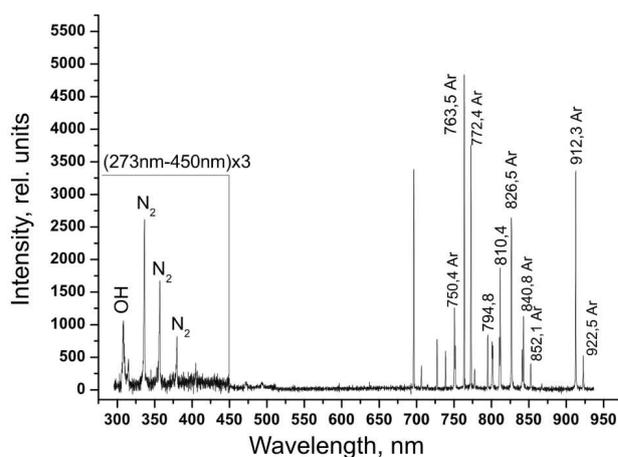

Fig. 2. Integrated-over-time emission spectrum of an argon plasma jet in the atmosphere registered at a distance of +3 mm from the capillary cut

lines dominates by intensity in the integrated radiation spectrum of the discharge plasma, amounting to not less than 90% of the total intensity. The same spectral interval also contains an insignificant, by intensity, emission of the spectral transition $3p\,^5P \rightarrow 3s\,^5S^0$ (at 777.4 nm) in oxygen atoms.

In the wavelength interval of 300–405 nm, the emission spectrum of a plasma jet is mainly presented by numerous spectral bands of nitrogen (Fig. 2) generated by electron-vibrational transitions of the second positive system of neutral nitrogen molecules. Besides the nitrogen emission, another band with the radiation intensity maximum at a wavelength of 308 nm was registered in the ultra-violet spectral range. It corresponds to the emission of hydroxyl radical OH (the $A\,^2\Sigma^+ \rightarrow X\,^2\Pi$ transition). The appearance of this band in the spectrum is connected with the process of dissociative excitation of water molecules,

Table 1. **Atomic and molecular emissions registered**
in the radiation spectrum of an atmospheric-pressure argon plasma jet

λ, nm	Plasma component	Electron (vibrational) transition	Excitation energy, eV	Intensity, rel. units
308	OH	$A^2\Sigma^+(v=0) \rightarrow X^2\Pi(v=0)$	9.1	7.3
315.9	N_2	$C^3\Pi_u(v=1) \rightarrow B^3\Pi_g(v=0)$	11.3	3.27
337.1	N_2	$C^3\Pi_u(v=0) \rightarrow B^3\Pi_g(v=0)$	11	18
357.7	N_2	$C^3\Pi_u(v=0) \rightarrow B^3\Pi_g(v=1)$	11	11.6
380.4	N_2	$C^3\Pi_u(v=0) \rightarrow B^3\Pi_g(v=2)$	11	5.6
405.8	N_2	$C^3\Pi_u(v=0) \rightarrow B^3\Pi_g(v=3)$	11	2.87
696.02	Ar	$3p^5(^2P^0_{1/2})4d^2[3/2]^0_2 \rightarrow 3p^5(^2P^0_{3/2})4s^2[3/2]_2$	14.95	70.01
706.7	Ar	$3p^5(^2P^0_{1/2})4p^2[3/2]_2 \rightarrow 3p^5(^2P^0_{3/2})4s^2[3/2]^0_2$	13.30	6.28
727.29	Ar	$3p^5(^2P^0_{1/2})4p^2[1/2]_1 \rightarrow 3p^5(^2P^0_{3/2})4s^2[3/2]^0_1$	13.32	16.6
738.39	Ar	$3p^5(^2P^0_{1/2})4p^2[3/2]_2 \rightarrow 3p^5(^2P^0_{3/2})4s^2[3/2]^0_1$	13.30	12.25
750.3	Ar	$3p^5(^2P^0_{1/2})4p^2[1/2]_0 \rightarrow 3p^5(^2P^0_{1/2})4s^2[1/2]^0_1$	13.47	26.01
763.51	Ar	$3p^5(^2P^0_{3/2})4p^2[3/2]_2 \rightarrow 3p^5(^2P^0_{3/2})4s^2[3/2]^0_2$	13.17	100
772.42	Ar	$3p^5(^2P^0_{1/2})4p^2[1/2]_1 \rightarrow 3p^5(^2P^0_{1/2})4s^2[1/2]^0_1$	13.32	77.7
777.4	O	$2p^3(^4S^0)2p^5P_2 \rightarrow 2p^3(^4S^0)3s^5S^0_2$	10.7	6.5
794.81	Ar	$3p^5(^2P^0_{3/2})4p^2[3/2]_1 \rightarrow 3p^5(^2P^0_{1/2})4s^2[1/2]^0_0$	13.28	17.5
800.61	Ar	$3p^5(^2P^0_{3/2})4p^2[3/2]_2 \rightarrow 3p^5(^2P^0_{3/2})4s^2[3/2]^0_1$	13.17	15.37
810.36	Ar	$3p^5(^2P^0_{3/2})4p^2[3/2]_1 \rightarrow 3p^5(^2P^0_{3/2})4s^2[3/2]^0_1$	13.15	38.74
826.45	Ar	$3p^5(^2P^0_{1/2})4p^2[1/2]_1 \rightarrow 3p^5(^2P^0_{1/2})4s^2[1/2]^0_1$	13.32	53.45
840.82	Ar	$3p^5(^2P^0_{3/2})4p^2[3/2]_2 \rightarrow 3p^5(^2P^0_{1/2})4s^2[1/2]^0_1$	13.30	23.3

which are present in air in the form of an atmospheric moisture:

$$H_2O + e \rightarrow OH(A^2\Sigma^+) + H + e. \qquad (1)$$
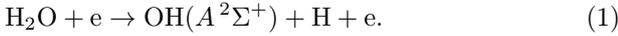
For the excited state $OH(A^2\Sigma^+)$ to appear as a result of the dissociative excitation of water molecules [Eq. (1)], an energy of about 9.1 eV is required [34], although the energy for this electron state to be excited from the ground one, $OH(X^2\Pi)$, amounts to only 4 eV. Despite that, under our conditions, hydroxyl molecules are mainly excited in the course of the dissociative excitation reaction of water molecules (1) because of the absence of hydroxyl radicals in the free state and because it is rather difficult to sufficiently accumulate them in the open space.

When looking through Table, one can clearly see that the molecular components of a plasma jet emit owing to the spectral transitions from the lowest vibrational energy levels of their electron states. This is an argument in favor of a rapid vibrational relaxation of excited molecules due to a high collision frequency of particles in the plasma at the atmospheric pressure.

The excitation energies for the top levels of various emitting transitions quoted in Table exceed 9 eV, which testifies to the presence of a considerable fraction of electrons with this energy in the discharge. However, it should be noted that high energy levels of molecules can be excited not only directly by electrons from the ground electron state owing to single collisions, but also as a result of multiple collisions through transient metastable states:

$$\begin{aligned} Ar + e &\rightarrow Ar^* + e, \\ Ar^* + e &\rightarrow Ar^{**} + e. \end{aligned} \qquad (2)$$

It is of interest to compare the results obtained in this work for the radiation spectrum of the argon plasma jet with our results obtained in work [35] for the radiation spectrum of a helium plasma jet under the same conditions. In the radiation spectrum of the former, the intensity of radiation given by spectral transitions of neutral atoms of the inert gas argon, which was blown through a capillary, is dominant. At the same time, the most intense lines in the radiation spectrum of a helium jet belong to the transitions of

the first negative system of molecular nitrogen ions N_2^+ $(B\,^2\Sigma_u^+ \to X\,^2\Sigma_g^+)$, with the radiation of neutral atoms of the inert gas helium being also rather intense. On the other hand, the spectral transitions of nitrogen ions are absent altogether from the radiation spectrum of the argon plasma jet.

In work [35], the assumption was made that the high intensity of radiation emission by molecular ions N_2^+ can result from a high efficiency of the Penning ionization process in the helium plasma at collisions of nitrogen molecules with metastable helium atoms, which gives rise to the formation of ions of nitrogen molecules in the ground and excited states $N_2^+(B\,^1\Sigma_u^+)$:

$$N_2(X\,^1\Sigma_g^+) + \mathrm{He}^* \to N_2^+(B\,^1\Sigma_u^+) + \mathrm{He} + e. \qquad (3)$$
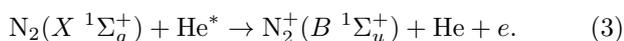
The results of researches carried out in this work confirmed the assumption made in work [34] about the main role of Penning processes in the formation of nitrogen ions and the excitation of intense radiation emission at the transitions of the first negative system of molecular nitrogen ions. As was mentioned above, the lines of molecular nitrogen ions are absent altogether from the radiation spectrum of the argon plasma jet, which is explained by the fact that nitrogen molecules are not ionized at their collisions with metastable argon atoms, because the energy of metastable argon atoms is insufficient for the Penning ionization process to take place. The minimum excitation energy for the ground electron state of a molecular nitrogen ion $N_2(X\,^2\Sigma_g^+)$ is equal to 15.6 eV, and the energy of the excited electron state $N_2^+(B\,^2\Sigma_u^+)$ amounts to 18.7 eV [28]. At the same time, the energies of the argon metastable states $3p^5(^2P_{3/2})4s\,^2[3/2]_2^0$ and $3p^5(^2P_{1/2})4s\,^2[1/2]_0^0$ equal 11.55 and 11.72 eV, respectively, which is not enough for the molecular nitrogen ions to be formed. Hence, the absence of the nitrogen-ion glowing in the argon plasma is a consequence of a very low efficiency of the formation of molecular nitrogen ions in the absence of such ionization channel as the Penning process. This conclusion confirms the assumption that it is the Penning process energetically allowed in the helium plasma (the energies of the lowest metastable states of a helium atom are 19.8 eV for $\mathrm{He}(1s2s\,^3S_1)$ and 20.6 eV for $\mathrm{He}(1s2s\,^1S_0)$ [26]), that gives rise to the effective ionization of nitrogen molecules and, consequently. to the intense glowing of transitions N_2^+ $(B\,^2\Sigma_u^+ \to X\,^2\Sigma_g^+)$.

Since, as was already mentioned above, the radiation spectrum of a plasma jet contains, besides the emissions of the inert gas argon, also other emissions associated with the accompanying excitation of atmospheric gases, studying the variations in the intensity of radiation emitted by the jet components along the propagation axis and finding the region, where the atmospheric gases mix with argon, are of importance. The spatial distribution of radiation was researched by measuring the radiation spectra at a number of points arranged along the plasma jet axis oriented horizontally. With the help of an optical lens, the plasma jet image was focused on the monochromator input slit. The jet image was moved across the slit by shifting the focusing optical lens along the jet axis. In this case, the monochromator input slit also played the role of an optical diaphragm and selected the radiation emitted from a certain jet section. In the experiment, its width was equal to 0.2 mm.

Besides the plasma spectral characteristics, we also studied the time dependences of plasma pulsed radiation parameters and evaluated the propagation velocity for the front of radiation emitted by the argon plasma and its nitrogen and hydroxyl components. The propagation velocity of the argon plasma was estimated as follows. Experimental oscillograms of the time evolution of radiation pulses emitted by the plasma components at various distances from the capillary cut were registered. Proceeding from the difference between the radiation pulse arrival times and the difference between the distances from the capillary cut, the velocity of motion for the front of radiation emitted by N_2 molecules and OH hydroxyl radicals was evaluated. According to the results of our measurements, it amounted to about 2000 m/s, with the velocity of argon outflow from the capillary being equal, as was already mentioned, to only 1 m/s. However, it should be noted that, according to the majority of researchers (see, e.g., work [36]), bright plasma formations (plasma balls) move in plasma jets along their axis with supersonic velocities up to several tens of km/s units. They are supposed to be generated in the barrier discharge. There is no common idea concerning the mechanism of their formation and acceleration. The most popular variant is that they are formed at the ionization wave front owing to the electron diffusion, ponderomotive force action, or breakdown waves.
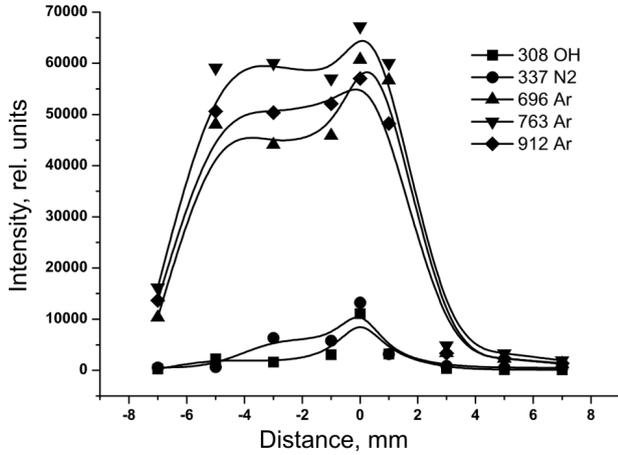
Fig. 3. Spatial distributions of the intensity for various spectral components in the radiation of an argon plasma jet

In Fig. 3, the spatial distributions of the radiation intensity are shown for some emissions of an atmospheric-pressure argon plasma jet. The space positions are reckoned from the capillary cut. The negative values of spatial coordinate correspond to scanning positions in the capillary depth. The most intense emissions correspond to the radiative transitions of N_2 $(C\ ^3\Pi_u[v=0] \to B\ ^3\Pi_g[v=0])$ at 337.1 nm, OH $(A\ ^2\Sigma^+[v=0] \to X\ ^2\Pi[v=0])$ at 308 nm, and O $(3p\ ^5P \to 3s\ ^5S^0)$ at 777.4 nm, as well as to the argon transitions $3p^5(^2P^0_{1/2})4d\ ^2[3/2]^0_2 \to 3p^5(^2P^0_{3/2})4p\ ^2[3/2]_2$ at 696 nm, $3p^5(^2P^0_{3/2})4p\ ^2[3/2]_2 \to 3p^5(^2P^0_{3/2})4s\ ^2[3/2]^0_2$ at 763.5 nm, and $3p^5(^2P^0_{3/2})4p\ ^2[1/2]_1 \to \to 3p^5(^2P^0_{3/2})4s\ ^2[3/2]^0_2$ at 912.3 nm.

All spatial distributions turned out to be of the same type for all plasma components. The highest intensities were observed at the capillary cut. At larger distances from the cut, the radiation intensities decreased on its both sides. We believe that the plasma jet obtains the most energy in the discharge gap of the barrier discharge in the form of excited and ionized components and electron gas. To a great extent, this energy is accumulated in the metastable states of argon with excitation energies of 11.55 and 11.72 eV and radiative lifetimes of 60 and 50 s, respectively [36]. However, following work [29], it should be noted that the effective lifetime for the group of excited states of the $3p^54s$ argon configuration, which includes the metastable $^3P_2$ and $^3P_0$ levels and the res-

onance $^3P_1$ and $^1P_1$ ones, is equal to about 10^{-2} s under the conditions of our experiment at atmospheric pressure. This value is determined by the processes of resonance radiation self-absorption and hybridization between the close electron states of argon. Those factors are quite enough for supporting the excitation processes of nitrogen molecules and hydroxyl radicals along the whole jet length. It is well known that metastable argon atoms can effectively enhance the radiation emissions of those objects by means of collisions of the second kind. At the same time, argon emissions can be excited, probably, by recombination processes. The presence of a substantial number of radiative transitions in an argon atom from the states with the energies considerably exceeding 11.72 eV (see Table) can probably mean that all radiative regularities are governed by two factors: the effective electron temperature and the concentrations of corresponding components. We think that, after its exit from the capillary into the atmosphere, the gas decelerates its translational propagation, so that some kind of a plug is formed here: a region with a raised concentration, where the radiation intensity maxima are observed. The further expansion results in a decrease of both the component concentrations and the electron temperature.

4. Conclusions

A plasma gas jet in the atmosphere is obtained by its excitation with the barrier discharge in a capillary, through which the inert gas argon is blown. The main emitting components of a plasma jet formed at the capillary output are excited argon and oxygen atoms, nitrogen molecules, and hydroxyl radicals. The radiation spectrum of a plasma jet is found to be mainly formed by radiative transitions between the excited states of argon and the transitions of the second positive system of nitrogen molecules. The propagation velocity of the radiation front emitted by N_2 molecules and hydroxyl radicals is evaluated to equal about 2000 m/s.

1. Kangil Kim, Geunyoung Kim, Yong Cheol Hong, and Sang Sik Yang, Microelectr. Eng. **87**, 1177 (2010).
2. M. Wolte, S. Bornholdt, M. Häckel, and H. Kersten, J. Achiev. Mater. Manufact. Eng. **37**, 730 (2009).
3. R. Foest, E. Kindel, A, Ohl, M. Stieber, and K.-D. Weltmann, Plasma Phys. Contr. Fus. **47**, B525 (2005).

4. A. Lehmann, A. Rueppell, A. Schindler, I.-M. Zylla, H.J. Seifert, F. Nothdurft, M. Hannig, and S. Rupf, Plasma Proc. Polym. **10**, 262 (2013).

5. A.C. Ritts, C.H. Liu, and Q.S. Yu, Thin Solid Films **519**, 4824 (2011).

6. L. Marcinauskas, M. Silinskas, and A. Grigonis, Appl. Surf. Sci. **257**, 2694 (2011).

7. Y. Hiroyuki, Rev. Sci. Instrum. **78**, 043510 (2007).

8. Li Haijiang, Wang Shouguo, Zhao Lingl, and Ye Tianchun, Plasma Sci. Technol. **6**, 2481 (2004).

9. M. Thiyagarajan, A. Sarani, and X. Gonzales, J. Appl. Phys. **113**, 093302 (2013).

10. Ye Tian, Peng Sun, Haiyan Wu, Na Bai, Ruixue Wang, Weidong Zhu, Jue Zhang, and Fuxiang Liu, J. Biomed. Res. **24**, 264 (2010).

11. Jae Koo Lee, Myoung Soo Kim, June Ho Byun, Kyong Tai Kim, Gyoo Cheon Kim, and Gan Young Park, Jpn. J. Appl. Phys. **50**, 08JF01 (2011).

12. J. Heinlin, G. Morfill, M. Landthaler, W. Stolz, G. Isbary, J.L. Zimmermann, T. Shimizu, and S. Karrer, J. Germany Soc. Dermatol. **8**, 1 (2010).

13. M. Laroussi, M.G. Kong, G. Morfill, and W. Stolz, *Plasma Medicine: Applications of Low-Temperature Gas Plasmas in Medicine and Biology* (Cambridge Univ. Press, Cambridge, 2012).

14. J. Raiser and M. Zenker, J. Phys. D **39**, 3520 (2006).

15. Jae-Hoon Kim, Mi-Ae Lee, Geum-Jun Han, and Byeong-Hoon Cho, Acta Odontol. Scand. **72**, 1 (2013).

16. Gyoo Cheon Kim, Hyun Wook Lee, June Ho Byun, Jin Chung, Young Chan Jeon, and Jae Koo Lee, Plasma Proc. Polym. **10**, 199 (2013).

17. Hyun Woo Lee, Seoul Hee Nam, A.-A.H. Mohamed, Gyoo Cheon Kim, and Jae Koo Lee, Plasma Proc. Polym. **7**, 274 (2010).

18. S. Lerouge, M.R. Wertheimer, and L'H.Yahia, Plasmas Polym. **6**, 175 (2001).

19. M. Moisan, J. Barbeau, M.-Ch. Crevier, J. Pelletier, N. Philip, and B. Saoudi, Pure Appl. Chem. **74**, 349 (2002).

20. Xiaoqing Dong, A.C. Ritts, C. Staller, Qingsong Yu, Meng Chen, and Yong Wang, Eur. J. Oral Sci. **121**, 355 (2013).

21. A.C. Ritts, Hao Li, Qingsong Yu, Changqi Xu, Xiaomei Yao, Liang Hong, and Yong Wang, Eur. J. Oral Sci. **118**, 510 (2010).

22. H.W. Herrmann, I. Henins, J. Park and G.S. Selwyn, Phys. Plasmas **6**, 2284 (1999).

23. M. Moravej, X. Yang, G.R. Nowling, J.P. Chang, R.F. Hicks, and S.E. Babayan, J. Appl. Phys. **96**, 7011 (2004).

24. Li Shou-Zhe, J.P. Lim, J.G. Kang, and H.S. Uhm, Phys. Plasmas **13**, 093503 (2006).

25. S. Wang, V. Schultz von der Gathen, and H.F. Dubele, Appl. Phys. Lett. **83**, 3272 (2003).

26. I.A. Soloshenko, V.V. Tsiolko, S.S. Pogulay, A.G. Terentyeva, V.Yu. Bazhenov, A.I. Shchedrin, A.V. Ryabtsev, and A.I. Kuzmichev, Plasma Sourc. Sci. Technol. **16**, 56 (2007).

27. I.A. Soloshenko, V.V. Tsiolko, S.S. Pogulay, A.G. Kalyuzhnaya, V.Yu. Bazhenov, and A.I. Shchedrin, Plasma Sourc. Sci. Technol. **18**, 1 (2009).

28. V.A. Khomich, A.V. Ryabtsev, E.G. Didyk, V.A. Zhovtyanskii, and V.G. Nazarenko, Pis'ma Zh. Tekhn. Fiz. **36**, 91 (2010).

29. V.A. Zhovtyanskii and O.V. Anisimova, Ukr. Fiz. Zh. **59**, 1155 (2014).

30. A.A. Radtsig and B.M. Smirnov, *Handbook on Atomic and Molecular Physics* (Atomizdat, Moscow, 1980) (in Russian).

31. http://physics.nist.gov/cgi-bin/ASD/lines1.pl.

32. R.R. Laher and F.R. Gilmore, J. Phys. Chem. Ref. Data **20**, 685 (1991).

33. K.P. Huber and G. Herzberg, *Molecular Spectra and Molecular Structure IV: Constants of Diatomic Molecules* (Van Nostrand, New York, 1979).

34. Y. Itikawa,and N. Mason, J. Phys. Chem. Ref. Data **34**, 1 (2005).

35. A.M. Korbut, V.A. Kelman, Yu.V. Zhmenyak, and M.S. Klenovskii, Opt. Spektrosk. **116**, 995 (2014).

36. A.A. Radtsig and B.M. Smirnov, *Reference Data on Atoms, Molecules, and Ions* (Springer, Berlin, 1986).

37. Jianun Shi, Fangchun Zhong, Jing Zhang, D.W. Liu, and M.G. Kong, Phys. Plasmas **15**, 013504 (2008).

О.М. Корбут, В.А. Кельман,
Ю.В. Жменяк, М.С. Кленівський

ЕМІСІЙНІ ВЛАСТИВОСТІ АРГОНОВОГО
ПЛАЗМОВОГО СТРУМЕНЯ АТМОСФЕРНОГО ТИСКУ
ЗІ ЗБУДЖЕННЯМ БАР'ЄРНИМ РОЗРЯДОМ

Р е з ю м е

Отримано плазмовий струмінь аргону в атмосфері шляхом збудження бар'єрного розряду в капілярній трубці, крізь яку продувався інертний газ аргон. Детально досліджено спектральний склад випромінювання аргонового плазмового струменя в атмосфері, а також просторово-спектральний розподіл інтенсивності його випромінювання. Показано, що спектральний склад випромінювання сформованого плазмового струменю представлений переважно спектральними переходами атомів аргону, кисню, а також електронно-коливними переходами першої позитивної системи молекул азоту $N_2(C\ ^3\Pi_u \rightarrow B\ ^3\Pi_g)$ та переходами радикалу гідроксилу $OH(A\ ^2\Sigma^+ \rightarrow X\ ^2\Pi)$.